

On the Limits of Highest-Occupied Molecular Orbital Driven Reactions: The Frontier Effective-for-Reaction Molecular Orbital Concept

Rodrigo R. da Silva,[†] Teodorico C. Ramalho,[†] Joana M. Santos,[‡] and J. Daniel Figueroa-Villar^{*,†}

Departamento de Química, Instituto Militar de Engenharia, Praça General Tibúrcio, 80, CEP 22290-070, Rio de Janeiro, Brazil, and Departamento de Química Geral e Inorgânica, Instituto de Química, Universidade do Estado do Rio de Janeiro, Rua São Francisco Xavier, 524, CEP 20550-013, Rio de Janeiro, Brazil

Received: August 8, 2005; In Final Form: November 2, 2005

We carried out Hartree–Fock (HF) and density functional theory calculations for 61 compounds, the conjugated bases of carboxylic acids, phenols, and alcohols, and analyzed their acid–base behavior using molecular orbital (MO) energies and their dependence on solvent effects. Despite the well-known correlation between highest-occupied MO (HOMO) energies and pK_a , we observed that HOMO energies are inadequate to describe the acid–base behavior of these compounds. Therefore, we established a criterion to identify the best frontier MO for describing pK_a values and also to understand why the HOMO approach fails. The MO that fits our criterion provided very good correlations with pK_a values, much better than those obtained by HOMO energies. Since they are the frontier molecular orbitals that drive the acid–base reactions in each compound, they were called frontier effective-for-reaction MOs, or FERMOs. By use of the FERMO concept, the reactions that are HOMO driven, and those that are not, can be better explained, independently from the calculation method used, as both HF and Kohn–Sham methodologies lead to the same FERMO.

1. Introduction

Computational Chemistry has attracted much attention in recent years due to the large and increasing interest in employing theoretical results for the analysis of recorded spectra as well as for the investigation of structure–property relationships and complementation of experimental data.¹ Theoretical approaches to compute structural and electronic parameters are now implemented in very efficient program packages that can be used in computing facilities with rapidly increasing performance.

The theoretical calculation of acid–base parameters, especially in solution, is a great challenge for quantum chemists. The calculation of gas-phase acid–base parameters has been a well-established methodology.¹ However, for solvated systems, this is not true. In fact, the aqueous medium is the most common one in chemical and biochemical processes; therefore, the calculation of acid–base parameters in aqueous solution has huge importance. Also, pK_a is the most useful acid–base parameter in aqueous solution, and many suggestions have been made in order to calculate accurate pK_a values.^{2–18}

Other works have shown how well pK_a values correlate with quantum descriptors. The average local ionization potential,^{19–21} atomic charges and interatomic distances,^{15,22–24} and the highest-occupied molecular orbital (HOMO) energy^{15,23,25–28} are the most common quantum descriptors used.

The relationships between HOMO energies and pK_a are often displayed for families of compounds, like phenols,²³ anilines,¹⁵ and azines.²⁶ However, for a number of other compounds, HOMO energies do not show good correlation with pK_a values,

and other quantum parameters, such as dipole moments, bond orders, atomic charges on hydrogens, and bond lengths, had to be included in a multiple linear regression analysis in order to improve the correlation.^{15,25,27,28} This procedure weakens the familiar idea that donor–acceptor reactions are driven by frontier orbital energies. Why are HOMO energies good acid–base descriptors for some compounds and not for others? Fujimoto and his group's work^{29,30,31} give some insight about this question. They had introduced the concept of localized reactive orbital (LRO), an orbital that is located on a reaction site and has as starting point an appropriate atomic orbital. They have shown that the delocalized nature of the HOMO fails to correctly describe reactions for some compounds and the LROs give better descriptions of those reactions.³⁰ The methodology developed for producing LROs was modified and improved by Hirao and Ohwada.³² Their method also provides a reactive orbital well localized around a reaction center and they called it as reactive hybrid orbital (RHO). They have showed that the RHO is much superior than HOMO to describe the electrophilic attack of a proton on an aromatic system.³² They also applied the RHO approach to other systems, such as carbonyl compounds,³³ cyclic amines,³⁴ and Diels–Alder reactions.³⁵ In all cases, RHO has described the reactivity of those compounds better than HOMO.

A careful study is necessary to understand when HOMO energy works and when it does not. Moreover there is a lack of studies concerning the most common and important organic acids, the carboxylic acids, and the relationship of their acid–base behavior with their MO energies. For this reason, our primary goal in this work was to investigate which is the best molecular orbital for describing the acid or base character for a collection of 36 carboxylic acids, 19 phenols, and 6 alcohols. We have also compared the use of Hartree–Fock (HF) and Kohn–Sham (KS) orbitals in this type of calculation.

* To whom correspondence should be addressed. E-mail: figueroa@ime.eb.br.

[†] Instituto Militar de Engenharia.

[‡] Universidade do Estado do Rio de Janeiro.

2. Theoretical Background on Molecular Orbitals

The major problem concerning the use of Schrödinger wave mechanics in chemistry is the lack of exact solutions for atoms or molecules that contain more than one electron. To solve that problem, there have been used approximations, such as the HF one.³⁶ By use of the HF and Roothaan–Hall equations in a self-consistent field (SCF) routine, one is able to calculate the electronic structure of a molecule,¹ which is represented by a group of wave functions ψ_a called molecular orbitals (MOs). The intensive development of the molecular orbital theory led to a greater understanding of chemistry and chemical reactions and, very recently, to a tomographic technique for imaging molecular orbitals.³⁷

Molecular orbitals and their properties, such as energies and symmetries, are very useful for chemists. The physical interpretation of the orbital energies was given by Koopmans.³⁸ Fukui and co-workers in their studies on reactivity of aromatic hydrocarbons³⁹ proposed the use of the frontier electron density for predicting the most reactive position on those systems. Their calculations were in excellent agreement with experimental data. Later, they have established some postulates, based on the frontier orbitals, for predicting the reactivity of π -electron systems in various types of reactions.⁴⁰ Also, Hoffmann and Woodward have developed a set of orbital symmetry rules that explained several types of reactions in conjugated systems.^{41–47} Later on, Salem also contributed for the development of the MO theory of conjugated systems.^{48,49} The MO theory was also successfully employed to describe Diels–Alder reactions,^{50–52} where the analysis of the HOMO–LUMO (lowest-unoccupied molecular orbital) interactions between the diene and the dienophile can be used to predict the promptness of a pericyclic reaction, as well as its stereo- and regioselectivity.

By exploration of Pearson's hard–soft acid–base (HSAB) concept,⁵³ Klopman proposed the concept of charge or frontier controlled reactions.⁵⁴ When the difference in energy between the HOMO of the donor and the LUMO of the acceptor is large, the reaction is charge controlled, and this is the nature of hard–hard interactions. On the other hand, if the difference is small, we have a frontier-controlled reaction and a soft–soft interaction. Other relation between the HSAB concept and molecular orbitals⁵⁵ is the following: the absolute hardness (η) of a given molecule is

$$\eta = \frac{E_{\text{LUMO}} - E_{\text{HOMO}}}{2} \quad (1)$$

Thus, soft acids or bases have small energy gaps between HOMOs and LUMOs, while hard ones have larger differences.

The idea of MOs in the HF–SCF procedure is quite natural, once MOs are the solutions for the HF equations. However, the concept of MOs in the density functional theory (DFT)^{56,57} is not simple to handle. In the DFT method, the variable which will determine all of the system properties is the total electron density, ρ , and not a wave function as in the HF approach. Therefore, the DFT orbitals, named KS orbitals, and the HF orbitals are, sometimes, treated as different quantum descriptors.⁵⁸ Another reason for that difference arises from the poor results given by the eigenvalues of KS orbitals in the description of the ionization potentials (IP) of molecules (the Koopmans' theorem). Politzer and Abu-Awwad have analyzed the behavior of HF and KS orbitals energies in many molecules and compared the results with the experimental IP,⁵⁹ showing that KS orbital energies differ significantly from experimental IP, while HF energies are in good agreement with them.

Nevertheless, those differences between HF and DFT approaches could be understood.^{58–60} Baerends and Gritsenko⁶⁰ pointed out that KS orbitals are suitable for being used in qualitative MO theory and that the problem with their energies comes from the poor asymptotic behavior of the available functionals.

In fact, the KS orbitals can be related to a number of chemical phenomena. Politzer and co-workers have shown the relation between HF and DFT average local ionization energies of monosubstituted benzene derivatives with the Hammett constants.⁶¹ Solomon and co-workers have shown that KS orbitals are related to the spectroscopic properties of inorganic compounds.^{62–69} The KS orbital eigenvalues, when obtained from the accurate density and true exchange–correlation potential, agree with the experimental excitation energies of He and Be atoms.⁷⁰ Stowasser and Hoffmann⁷¹ made another comparison between HF and KS orbitals. They found that KS orbitals are suitable for qualitative MO analyses, as described by Baerends and Gritsenko⁶⁰ but that a quantitative interpretation is more difficult.

3. Methods

3.1. Computational Details. All calculations were carried out with the Gaussian 98 package.⁷² Each conjugated base from all 61 compounds was fully optimized using DFT with the B3LYP functional^{73,74} employing the 6-31G(d,p) basis set. No symmetry constraint was imposed during the optimization process. No imaginary frequencies were found for the optimized geometries. These optimized geometries were used in all subsequent calculations. HF single-point energy calculations were computed using the 6-31G(d,p) basis set.

To account for solvent effects from water, single-point energy calculations were obtained using the polarizable continuum model (PCM)^{75–77} and the conductorlike screening model (COSMO)^{78,79} at both DFT/B3LYP and HF level with the 6-31G(d,p) and 6-31+G(d,p) basis sets. The orbital energies from these methods were fit to a linear model with experimental pK_a values. The determination coefficients (r^2) and other statistical parameters were analyzed and compared.

The MOs figures were prepared using the Gaussian View 2.1 package⁷² using a contour value of 0.020.

3.2. Orbital Choice Criteria. It is well known that Brønsted–Lowry acid–base reactions are localized phenomena, which take place between the proton and one atom (or a group of atoms) in a molecule. Therefore, the MO which drives those reactions must be centered in this atom or group of atoms and also be a frontier MO. We carried out the investigation of these orbitals in two different ways: by looking at the orbital shapes⁸⁰ and by calculating the MOs composition using the expansion coefficients.

4. Results and Discussion

4.1. Carboxylic Acids. Table 1 shows the 36 carboxylic acids used in this work and their experimental pK_a values for the reaction



4.1.1. The HOMO Problem. We started our analysis using HOMO energies as a quantum descriptor for the pK_a values as described for other compounds.^{15,23,25–28} However, the results at all levels of calculation⁸² for carboxylate ions were disappointing (Table 2). The statistical Fisher test ($F_{1,30} = 7.56$, 99% confidence level)⁸³ was used to evaluate the significance of the

TABLE 1: Substituted Carboxylic Acids and Their Experimental pK_a Values

| | carboxylic acids | pK_a | ref |
|----|-------------------------------|--------|-----|
| 1 | 2,2-dimethyl-propionic acid | 5.05 | 16 |
| 2 | propionic acid | 4.87 | 16 |
| 3 | butyric acid | 4.82 | 16 |
| 4 | acetic acid | 4.76 | 16 |
| 5 | <i>p</i> -methyl-benzoic acid | 4.37 | 24 |
| 6 | vinyl-acetic acid | 4.35 | 16 |
| 7 | phenyl-acetic acid | 4.31 | 16 |
| 8 | <i>m</i> -methyl-benzoic acid | 4.27 | 24 |
| 9 | succinic acid | 4.21 | 81 |
| 10 | benzoic acid | 4.19 | 24 |
| 11 | <i>p</i> -fluoro-benzoic acid | 4.14 | 24 |
| 12 | 3-chloro-propionic acid | 4.10 | 16 |
| 13 | <i>p</i> -chloro-benzoic acid | 3.98 | 24 |
| 14 | <i>p</i> -bromo-benzoic acid | 3.97 | 24 |
| 15 | <i>m</i> -fluoro-benzoic acid | 3.87 | 24 |
| 16 | <i>m</i> -chloro-benzoic acid | 3.83 | 24 |
| 17 | glycolic acid | 3.83 | 16 |
| 18 | <i>m</i> -bromo-benzoic acid | 3.81 | 24 |
| 19 | formic acid | 3.75 | 16 |
| 20 | <i>m</i> -cyano-benzoic acid | 3.60 | 24 |
| 21 | <i>p</i> -cyano-benzoic acid | 3.55 | 24 |
| 22 | methoxy-acetic acid | 3.54 | 16 |
| 23 | 3-butynoic acid | 3.32 | 16 |
| 24 | fumaric acid | 3.05 | 81 |
| 25 | bromo-acetic acid | 2.86 | 16 |
| 26 | malonic acid | 2.85 | 81 |
| 27 | chloro-acetic acid | 2.81 | 16 |
| 28 | 2-chloro-propionic acid | 2.80 | 16 |
| 29 | fluoro-acetic acid | 2.66 | 16 |
| 30 | cyano-acetic acid | 2.44 | 16 |
| 31 | nitro-acetic acid | 1.32 | 16 |
| 32 | dichloro-acetic acid | 1.30 | 16 |
| 33 | oxalic acid | 1.25 | 81 |
| 34 | difluoro-acetic acid | 1.24 | 17 |
| 35 | trichloro-acetic acid | 0.63 | 17 |
| 36 | trifluoro-acetic acid | 0.23 | 17 |

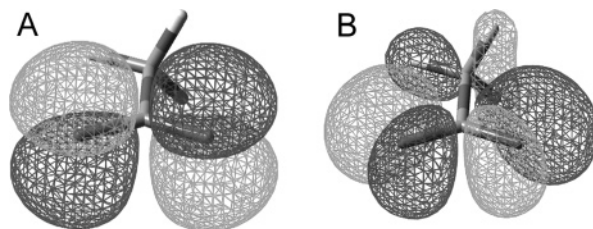
linear model, and it was found that none of those regressions could be considered as a linear model. To be considered statistically significant, a linear model must have an F value at least 10 times higher than the Fisher F value. Although we have 34 degrees of freedom, we are using the value for 30.

Some questions arose from these poor results. The first one is: are the basis sets used adequately? Nowadays, the 6-31G(d,p) and the 6-31+G(d,p) basis sets are relatively simple; however, they have been used in other works to predict pK_a values and the results were satisfactory.^{7,8,11,16} Also, Schüürmann and co-workers have compared the performance of some basis sets to predict pK_a values. They have found that the 6-31G(d,p) and 6-31+G(d,p) basis sets gave better values than more complex ones.⁶ Accordingly, we believe that the basis set size alone cannot justify the poor correlation between HOMO energies of these carboxylate ions and their pK_a values. This takes us to the second question: is the HOMO the best orbital for describing the acid–base character of those compounds? To answer that question, we had to go deeper into MO properties.

TABLE 2: Linear Regression Parameters for pK_a Values vs HOMO Energy^a Plots Calculated by Different Methods and Basis Sets for Carboxylate Ions

| methodology | r^2 | a^b | b^c | pK_a error | SD ^d | F |
|-----------------------|-------|--------------|-------------|--------------|-----------------|------|
| HF/6-31G(d,p) | 0.468 | 52.7 (17.8) | 13.2 (3.4) | 1.75 | 0.924 | 29.9 |
| HF/COSMO/6-31G(d,p) | 0.448 | 28.5 (13.5) | 13.7 (4.9) | 2.38 | 0.941 | 27.6 |
| HF/COSMO/6-31+G(d,p) | 0.383 | 22.9 (13.3) | 12.1 (5.1) | 2.69 | 0.996 | 21.1 |
| DFT/6-31G(d,p) | 0.309 | 39.7 (19.6) | 4.39 (0.62) | 2.07 | 1.05 | 15.2 |
| DFT/COSMO/6-31G(d,p) | 0.542 | 92.7 (21.2) | 23.9 (4.7) | 1.29 | 0.857 | 40.3 |
| DFT/COSMO/6-31+G(d,p) | 0.638 | 103.2 (19.0) | 29.7 (4.9) | 1.13 | 0.762 | 60.0 |

^a Values for orbitals energies in Hartrees. ^b Angular coefficient. The number in parentheses is the standard error. ^c Linear coefficient. The number in parentheses is the standard error. ^d SD = standard deviation or root-mean-square deviation. $F_{1,30} = 7.56$, 99% confidence level.

**Figure 1.** Surface plots for the acetate HOMO. (A) HF method (p_z -type) and (B) DFT method ($p_x p_y$ -type).

4.1.2. Behavior of HF and KS Orbitals. When comparing HF and KS orbitals, the first thing that was noticed, for the conjugated bases used, was that the shape of the HOMO orbitals given by the HF method were different from the ones obtained by the DFT method, as shown for acetate ion in Figure 1. By use of acetate as an example, it is observed that the main contribution for the HOMO calculated with the HF method comes from oxygen p_z atomic orbitals. On the other hand, the HOMO calculated with DFT has a strong contribution from the oxygen p_x and p_y atomic orbitals. For this reason, we will refer these orbitals as p_z -type (Figure 1A) and $p_x p_y$ -type (Figure 1B).⁸⁴ It must be noticed that the $p_x p_y$ -type MO is present in the HF set of orbitals for acetate, in the same way that the p_z -type is present among the KS orbitals. That is, the p_z - and $p_x p_y$ -type MOs are obtained by both HF and DFT methods, with roughly the same shape, but with different energy orders. For example, for acetate ion, the p_z -type orbital is the HF HOMO orbital, while the $p_x p_y$ -type orbital is the DFT HOMO. The same behavior is observed for all of other 35 carboxylate ions. Figure 2 shows p_z and $p_x p_y$ -type MOs for other carboxylic acid conjugated bases. Interestingly, this type of behavior between HF and KS orbitals has been observed for other molecules.⁷¹ For several compounds, when solvent effects are considered, the MO energy positions relative to the one observed in a vacuum are interchanged.⁸² This variation on MO energy positions is also observed when different basis sets are used.⁸²

Independent from the orbital energy order changes, there is a constant feature for those orbitals. In HF calculations, p_z -type MOs have always had higher energies than $p_x p_y$ -type ones, while in DFT calculations the opposite energy order is always found. Since p_z and $p_x p_y$ -type MOs are observed for all the studied compounds by all of the calculation methods, and considering that both types of orbitals are mainly located at the carboxylate moiety, they meet our orbital choice criterion for describing the acid–base character of a given molecule, as discussed before. Accordingly, we have investigated if those MO energies are better pK_a descriptors than HOMO energies.

4.1.3. Correlation between p_z - and $p_x p_y$ -Type MO Energies and pK_a Values. We have carried out the same analysis for p_z and $p_x p_y$ -type MO energies correlation with pK_a , as it was done for the HOMO energies, that is, using the statistical Fisher test. Table 3 shows the results for the different methodologies using p_z -type MO energies as a quantum descriptor for pK_a values.⁸²

TABLE 3: Linear Regression Parameters for pK_a Values vs p_z -Type MO Energy^a Plots

| methodology | r^2 | a^b | b^c | pK_a error | SD ^d | F |
|-----------------------|-------|--------------|-------------|--------------|-----------------|-------|
| HF/6-31G(d,p) | 0.459 | 55.3 (18.5) | 13.8 (3.5) | 1.72 | 0.932 | 28.8 |
| HF/COSMO/6-31G(d,p) | 0.812 | 145.0 (15.3) | 61.3 (6.1) | 0.74 | 0.550 | 146.4 |
| HF/COSMO/6-31+G(d,p) | 0.862 | 179.7 (14.4) | 79.5 (6.1) | 0.58 | 0.471 | 212.6 |
| DFT/6-31G(d,p) | 0.285 | 40.7 (20.6) | 4.99 (0.90) | 2.04 | 1.07 | 13.6 |
| DFT/COSMO/6-31G(d,p) | 0.809 | 137.3 (15.0) | 36.4 (3.6) | 0.76 | 0.554 | 143.9 |
| DFT/COSMO/6-31+G(d,p) | 0.851 | 184.0 (15.2) | 55.0 (4.3) | 0.60 | 0.489 | 194.7 |

^a Values for orbitals energies in Hartrees. ^b Angular coefficient. The number in parentheses is the standard error. ^c Linear coefficient. The number in parentheses is the standard error. ^d SD = standard deviation or root meansquare deviation. $F_{1,30} = 7.56$, 99% confidence level.

TABLE 4: Linear Regression Parameters for pK_a Values vs p_xp_y -Type MO Energy^a Plots

| methodology | r^2 | a^b | b^c | pK_a error | SD ^d | F |
|-----------------------|--------------------|--------------|------------|--------------|-----------------|-------|
| HF/6-31G(d,p) | 0.523 | 54.6 (16.7) | 14.8 (3.5) | 1.68 | 0.875 | 37.3 |
| HF/COSMO/6-31G(d,p) | 0.920 | 126.0 (9.0) | 55.5 (3.7) | 0.53 | 0.358 | 391.0 |
| HF/COSMO/6-31+G(d,p) | 0.814 ^e | 130.1 (14.4) | 60.2 (6.3) | 0.77 | 0.547 | 148.8 |
| DFT/6-31G(d,p) | 0.309 | 39.7 (19.6) | 4.4 (0.6) | 2.07 | 1.05 | 15.2 |
| DFT/COSMO/6-31G(d,p) | 0.871 | 127.6 (11.7) | 32.3 (2.7) | 0.66 | 0.455 | 230.3 |
| DFT/COSMO/6-31+G(d,p) | 0.928 | 147.4 (9.2) | 42.2 (2.4) | 0.47 | 0.340 | 438.5 |

^a Values for orbitals energies in Hartrees. ^b Angular coefficient. The number in parentheses is the standard error. ^c Linear coefficient. The number in parentheses is the standard error. ^d SD = standard deviation or root-mean-square deviation. ^e Compound **35** is an outlier, see text. $F_{1,30} = 7.56$, 99% confidence level.

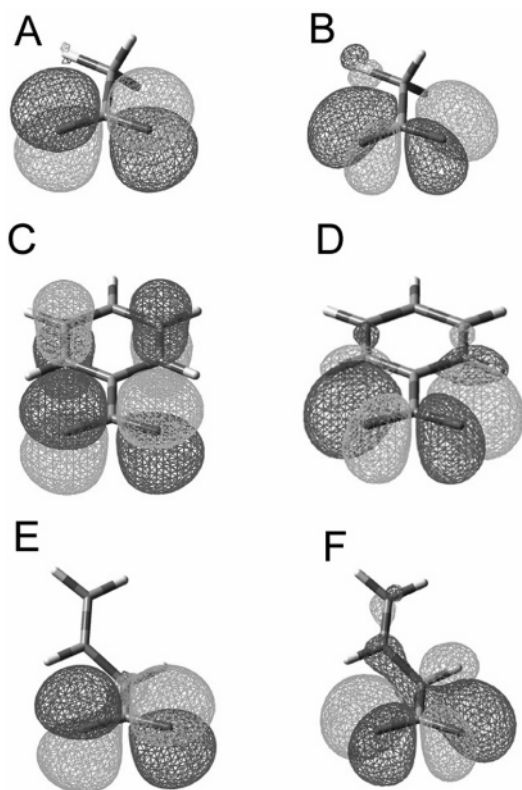


Figure 2. Surface plots for p_z - and p_xp_y -type MOs for some other carboxylic acid conjugated bases at HF level: fluoro-acetate p_z (A) and p_xp_y -type (B) MOs; benzoate p_z (C) and p_xp_y -type (D) MOs; vinyl-acetate p_z (E) and p_xp_y -type (F) MOs.

Although the results using p_z -type MO energies show a significant improvement when compared to HOMO energies, they still have large deviations from the ideal linear model. It is important to notice that the methodologies that did not consider solvent effects provided very low F values and could not be considered as linear models. On the other hand, the methodologies HF/COSMO/6-31G(d,p) and DFT/COSMO/6-31+G(d,p) yielded the best linear regression parameters, thus reinforcing the importance of solvent effects on this type of calculation.

The results from p_xp_y -type MOs are shown in Table 4. The same behavior displayed by the p_z -type MOs case was observed for the p_xp_y -type MOs, that is, the methodologies without solvent effects yielded poor F values and showed no statistical significance. Again, the methodologies HF/COSMO/6-31G(d,p) and DFT/COSMO/6-31+G(d,p) provided the best linear regression parameters. From the results, it is clear that solvent effects have a central role in acid–base behavior and that orbital energies are sensitive to them. The pK_a values are related to the ΔG° for the proton-transfer reaction in aqueous solution ($\Delta G^\circ_{(aq)}$). $\Delta G^\circ_{(aq)}$ is a function of enthalpy ($\Delta H^\circ_{(aq)}$) and entropy ($\Delta S^\circ_{(aq)}$), and in solution the entropy term is usually determinant for the pK_a values.⁸⁵ Since this is the case for carboxylic acids,⁸⁶ a solvation model is necessary to correctly describe the pK_a variation along the collection of carboxylate ions. However, for other works that correlate MO energies with pK_a values^{15,23,26} the solvent effects were neglected. That approximation was valid as all of the systems studied before (anilines,¹⁵ phenols,²³ and azines²⁶) have an aromatic ring in their structure, and as a consequence, their sizes and their geometries do not vary strongly. For these reasons, the entropy term may be roughly the same along each of these families of compounds and the solvent effects will also be leveled.

As it can be observed from the results shown in Tables 3 and 4, only for one methodology (HF/COSMO/6-31+G(d,p)) the correlation parameters were better for the p_z -type MOs than for the p_xp_y -type MOs. However, in the p_xp_y -type MOs linear regression, compound **35** (trichloroacetate ion) is an outlier.⁸⁷ Without this point, the r^2 value increases from 0.814 to 0.898 for the p_xp_y -type MOs correlation, which is a better determination coefficient value than the one obtained for the p_z -type MOs.

The better pK_a description given by p_xp_y -type MO energies in relation to p_z -type MO and HOMO energies is shown in Figure 3. The plots **A** and **D** in Figure 3 are pK_a and HOMO energies correlations for HF and DFT methods, respectively. Plots **C** and **F** are pK_a correlations using p_xp_y -type MO energies for HF (**C**) and DFT (**F**) methods. Plot **B** shows the correlation between pK_a and p_z -type MO energies for HF and plot **E** shows the same correlation for the DFT method. The improvement on the correlations when other MO energies are used instead

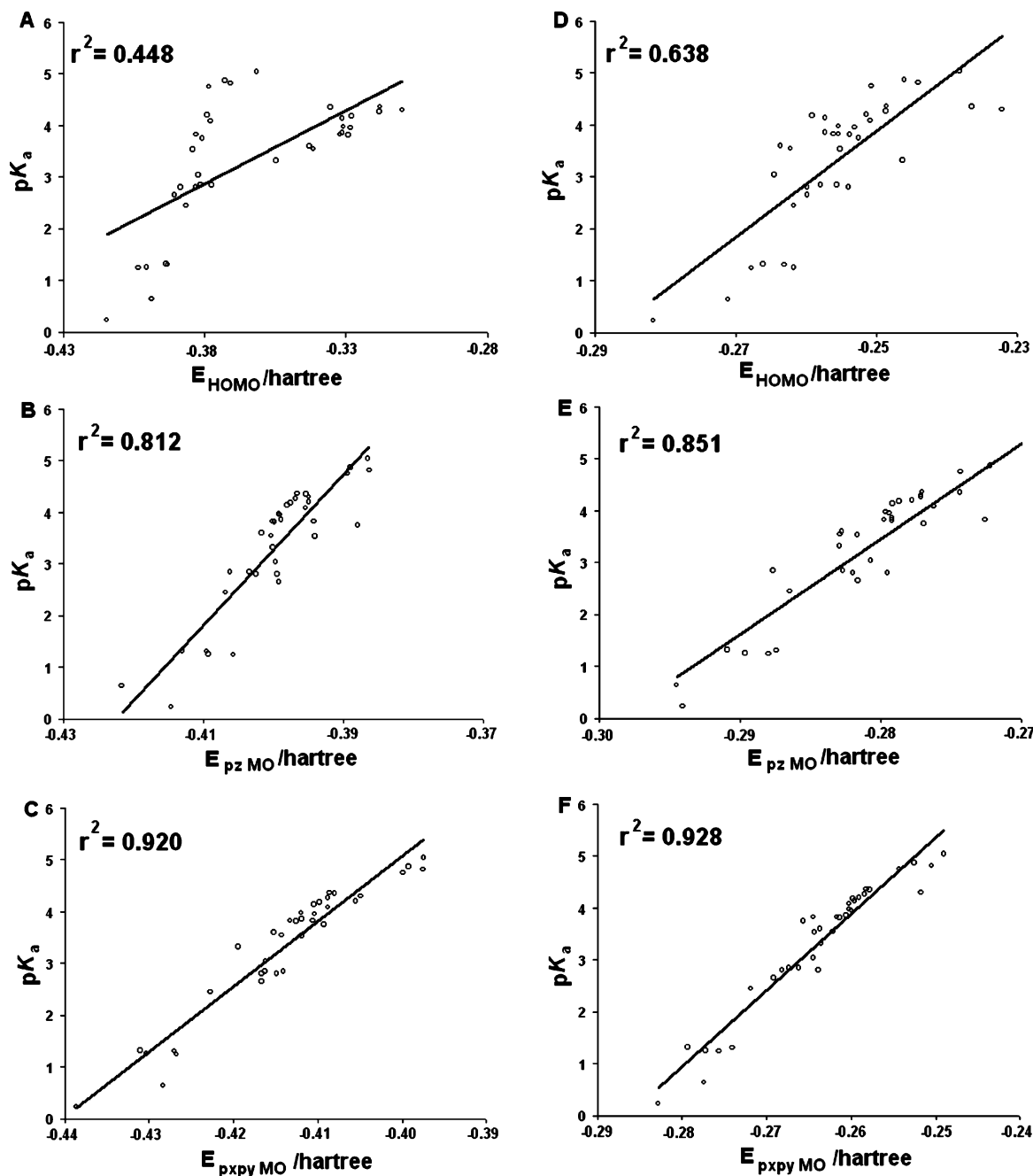


Figure 3. Plots for the correlation between the carboxylic acids pK_a values and carboxylate ions MO energies (in hartree). (A) HF HOMO; (B) HF p_z -type MO; (C) HF p_xp_y -type MO; (D) DFT HOMO; (E) DFT p_z -type MO; (F) DFT p_xp_y -type MO. MO energies for plots A, B, and C were calculated at HF/COSMO/6-31G(d,p) level and for plots D, E, and F were calculated at DFT/COSMO/6-31+G(d,p) level.

of HOMO energies is clearly shown by the plots. It is also interesting to notice that HF and KS MOs behave in a very similar way.

The results shown in Tables 3 and 4 and Figure 3 take us to a key question: why are p_xp_y -type MO energies better quantum descriptors for pK_a values than p_z -type MO ones? The answer to this question resides in the shape of those MOs. It is well known that the carboxylic acid moiety from these acids has a planar geometry.^{12,13,24,88} This is a restriction for proton-transfer reactions within those species, since the proton must lie on the plane of the carboxylate moiety, otherwise the sigma O–H bond cannot be formed. Moreover, when a carboxylic acid loses its acidic proton, the electrons from the broken O–H bond will be on the same plane of the former sigma bond, i.e., the carboxylate moiety plane. Another important factor regarding the basicity of carboxylate ions is the resonance that exists within their

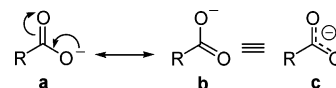


Figure 4. Resonance structures of a carboxylate ion.

carboxylate moiety (Figure 4),⁸⁹ which explains its planar geometry. Thus, many important factors concerning the proton transfer in those compounds are related to the carboxylate plane.

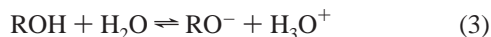
We can now make a statement about the question related with the p_z - and p_xp_y -type MO correlation with pK_a . It is clear that p_z -type MOs have a horizontal nodal plane that coincides with the carboxylate plane while the p_xp_y -type MOs have only perpendicular nodal planes (see Figures 1 and 2). The σ bond between the hydrogen unoccupied 1s orbital and the electron-donor carboxylate MO cannot be formed at the position in which this carboxylate MO has a nodal plane. Because of that, the

TABLE 5: Phenols and Aliphatic Alcohols and Their Experimental pK_a Values

| | compound | pK_a | ref |
|----|--------------------------|--------|-----|
| 37 | <i>t</i> -butanol | 18.0 | 14 |
| 38 | isopropanol | 17.1 | 8 |
| 39 | <i>n</i> -propanol | 16.1 | 8 |
| 40 | ethanol | 15.9 | 8 |
| 41 | methanol | 15.5 | 8 |
| 42 | 2,2,2-trifluoro-ethanol | 12.5 | 55 |
| 43 | <i>p</i> -amino-phenol | 10.30 | 23 |
| 44 | <i>p</i> -methoxy-phenol | 10.21 | 23 |
| 45 | <i>p</i> -methyl-phenol | 10.14 | 23 |
| 46 | <i>m</i> -methyl-phenol | 10.08 | 23 |
| 47 | phenol | 9.98 | 23 |
| 48 | <i>p</i> -hydroxy-phenol | 9.96 | 23 |
| 49 | <i>p</i> -fluoro-phenol | 9.95 | 23 |
| 50 | <i>m</i> -amino-phenol | 9.87 | 23 |
| 51 | <i>m</i> -methoxy-phenol | 9.65 | 23 |
| 52 | <i>m</i> -hydroxy-phenol | 9.44 | 23 |
| 53 | <i>p</i> -chloro-phenol | 9.38 | 23 |
| 54 | <i>p</i> -bromo-phenol | 9.36 | 23 |
| 55 | <i>m</i> -fluoro-phenol | 9.28 | 23 |
| 56 | <i>m</i> -bromo-phenol | 9.03 | 23 |
| 57 | <i>m</i> -chloro-phenol | 9.02 | 23 |
| 58 | <i>m</i> -cyano-phenol | 8.61 | 23 |
| 59 | <i>m</i> -nitro-phenol | 8.40 | 23 |
| 60 | <i>p</i> -cyano-phenol | 7.95 | 23 |
| 61 | <i>p</i> -nitro-phenol | 7.15 | 23 |

p_z -type MOs cannot form a σ bond in the carboxylate plane. Therefore, p_x, p_y -type MOs will be the ones related with the electron-donor properties of those carboxylate ions, that is, they must be the MOs that drive acid–base reactions in the system carboxylic acids/carboxylate ions.

4.2. Phenols and Alcohols. To test the previous idea with other acids, we decided to try a set of compounds with a group different from the carboxylate, the hydroxyl one. To make the test even more comprehensive, several phenols and alcohols were included in the new set of compounds, which are listed, together with their pK_a values, in Table 5. The studied acid–base reaction is



4.2.1. HOMO Problem. As it was observed previously for the carboxylic acids, there is a problem with the correlation of HOMO with pK_a for those compounds. However, the problem

here is quite different. Again, the statistical Fisher test ($F_{1,23} = 7.88$, 99% confidence level) was employed to evaluate the significance of the linear model for the correlation of the HOMO energy with pK_a . Phenoxide and alkoxide ions together provided very poor linear models (Table 6).⁸² The only exception was the methodology DFT/6-31G(d,p), which gave acceptable determination coefficients and F values, but also high standard deviations and pK_a errors. Therefore, the results obtained for some regression parameters with the DFT/6-31G(d,p) methodology are much more of a coincidence than a reliable linear model behavior. On the other hand, if we consider them as two separate classes of compounds, phenoxide ions (Table 7)⁸² and alkoxide ions, the correlations between HOMO energies and pK_a values are satisfactory. Although the correlation between alkoxide HOMO energies and pK_a yielded good linear regression parameters (with solvent effects, the r^2 values ranged from 0.859 to 0.979), the number of compounds is too small to build a solid statistical linear model. Therefore, the correlation parameters are not shown here.

The correlation between phenoxide ions HF HOMO energies and pK_a values has been reported by Gross and Seybold,²³ but the authors found a poor correlation at the DFT level. We, on the contrary, have found that the correlations between HOMO energies at the DFT level and pK_a values were as good as those found at HF level. The optimization methodology adopted here does not differ significantly from the one adopted by Gross and Seybold. Therefore, the differences between our and their results do not come from the equilibrium geometry. However, the basis set they used to calculate the MO energies, 6-311G(d,p), was different from the basis set we used. Since this is the main methodological difference between both works, we believe that their poor results at the DFT level may be due to the dependence between the MO energy positions and the basis sets (see discussion above, on topic 4.1.2).

Interestingly, the correlation parameters for phenoxide ions are slightly better without the inclusion of solvent effects. As previously discussed, we believe that since the size and geometry of these molecules do not vary significantly, the solvent effects would be roughly the same for all compounds, except for those with very polar groups such as OH and NH₂. For that reason, for phenoxide ions, the solvent effects could be suppressed, keeping the correlation between HOMO energies and pK_a values still satisfactory.

TABLE 6: Linear Regression Parameters for pK_a Values vs HOMO Energy^a Plots for Phenoxide and the Alkoxide Ions

| methodology | r^2 | a^b | b^c | pK_a error | SD ^d | F |
|-----------------------|-------|---------------|--------------|--------------|-----------------|-------|
| HF/6-31G(d,p) | 0.001 | 5.82 (60.1) | 11.4 (5.0) | 5.17 | 3.11 | 0.02 |
| HF/COSMO/6-31G(d,p) | 0.637 | -69.5 (25.1) | -7.84 (6.82) | 4.40 | 1.87 | 40.3 |
| HF/COSMO/6-31+G(d,p) | 0.679 | -65.1 (22.4) | -7.87 (6.53) | 4.33 | 1.76 | 48.6 |
| DFT/6-31G(d,p) | 0.828 | 92.6 (18.6) | 9.14 (0.65) | 2.81 | 1.29 | 110.8 |
| DFT/COSMO/6-31G(d,p) | 0.016 | 38.4 (76.5) | 17.2 (12.6) | 4.11 | 3.09 | 0.386 |
| DFT/COSMO/6-31+G(d,p) | 0.230 | -110.6 (59.4) | -10.5 (11.5) | 4.08 | 2.73 | 6.87 |

^a Values for orbitals energies in Hartrees. ^b Angular coefficient. The number in parentheses is the standard error. ^c Linear coefficient. The number in parentheses is the standard error. ^d SD = standard deviation or root-mean-square deviation. $F_{1,23} = 7.88$, 99% confidence level.

TABLE 7: Linear Regression Parameters for pK_a Values vs HOMO Energy^a Plots for Phenoxide Ions

| methodology | r^2 | a^b | b^c | pK_a error | SD ^d | F |
|-----------------------|-------|-------------|-------------|--------------|-----------------|-------|
| HF/6-31G(d,p) | 0.953 | 48.7 (3.7) | 13.2 (0.3) | 0.29 | 0.188 | 345.6 |
| HF/COSMO/6-31G(d,p) | 0.880 | 77.9 (7.6) | 28.9 (1.9) | 0.37 | 0.300 | 125.0 |
| HF/COSMO/6-31+G(d,p) | 0.858 | 82.1 (8.6) | 31.4 (2.3) | 0.40 | 0.326 | 102.8 |
| DFT/6-31G(d,p) | 0.949 | 45.4 (3.8) | 9.10 (0.07) | 0.31 | 0.196 | 315.0 |
| DFT/COSMO/6-31G(d,p) | 0.929 | 75.1 (5.7) | 21.6 (0.9) | 0.29 | 0.230 | 223.4 |
| DFT/COSMO/6-31+G(d,p) | 0.949 | 145.6 (6.6) | 44.3 (1.6) | 0.20 | 0.195 | 319.0 |

^a Values for orbitals energies in Hartrees. ^b Angular coefficient. The number in parentheses is the standard error. ^c Linear coefficient. The number in parentheses is the standard error. ^d SD = standard deviation or root-mean-square deviation. $F_{1,17} = 8.40$, 99% confidence level.

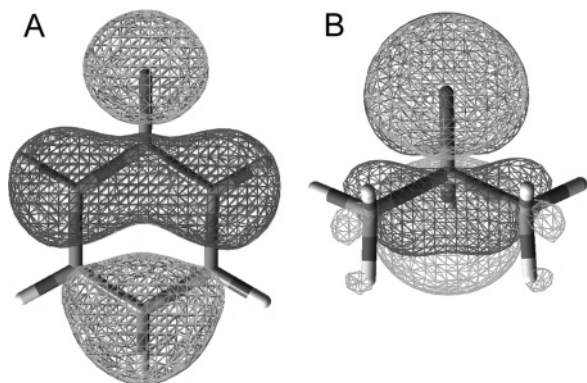


Figure 5. Surface plots for the HOMO at DFT level for the phenoxide ion (A) and the isopropoxide ion (B) anions.

Despite the reasonable results obtained for phenols and alcohols conjugated bases as independent groups, they should be considered as only one group, as they have the same acid/base group, the OH/O⁻. Having the same acid/base group implies that acid–base reactions will be driven by a MO common to both alkoxide and phenoxide ions. We have just shown that the HOMO is not this common orbital, since its energy cannot describe the acid–base behavior of alcohols and phenols as a single group. The question now is which MO should be used to unify them into a single group?

4.2.2. Behavior of HF and KS Orbitals. Once again, by looking at the MO shapes, the HOMO problem can be better understood. In fact, we can see that phenols and alcohols are part of the same group. Differently from carboxylate ions, for phenoxide and alkoxide ions the HOMO shape from HF and DFT calculations is the same, with the methoxide and *t*-butoxide ions being the only exceptions, where the HF HOMO are DFT second highest occupied molecular orbital and vice versa.

Figure 5 shows the HOMO shapes for the phenoxide and isopropoxide ions. As it can be noticed, in the phenoxide ion (Figure 5A), the HOMO orbital is under strong influence from the aromatic π -electrons. This influence is present in the HOMO of all of the phenoxide ions used in this study. On the other hand, the alkoxide ion HOMOs do not have this influence (Figure 5B). This is why the HOMO energy cannot describe both alcohols and phenols as a single acid/base group. Interestingly, the alcohols anions have another MO whose energy is very close to their HOMO energy. These almost degenerate MOs (actually degenerate for the methoxide and the *t*-butoxide ions) can also be labeled as p_z -type for the HOMO and p_xp_y -type for the second HOMO. More interestingly, the phenoxide ions also possess the p_xp_y -type MOs as observed for alkoxide ions. Figure 6 shows the p_xp_y -type MO for phenoxide ion (A) and isopropoxide ion (B). However, for phenoxide ions, the energy difference between the HOMO (p_z -type MO) and the p_xp_y -type MO (third HOMO at HF level and often the second HOMO at the DFT) are quite large when compared with those differences observed for alkoxide ions.⁸² The energy difference observed

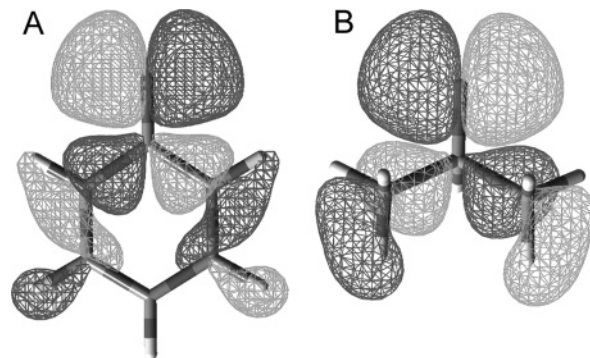


Figure 6. Surface plots for p_xp_y -type MO at the DFT level for the phenoxide ion (A) and the isopropoxide ion (B) anions.

for those two MOs in phenoxide ions is clearly due to the aromatic π -electron influence in the HOMO (Figure 5A), which is not present in the p_xp_y -type MO (Figure 6A).

The HOMO problem arises from the influence of the aromatic π -electrons, and the solution would be finding a MO that does not have this influence. Thus, the p_xp_y -type MOs became a natural choice to solve this problem. Moreover, they also fit our orbital choice criterion, because they are common to all of the studied compounds and are mainly located where the reaction takes place, at the oxygen atom. Are the p_xp_y -type MO the frontier MO that drives the protonation reaction for both alkoxide and phenoxide ions?

4.2.3. Correlation of p_xp_y -Type MO Energies and pK_a Values of Phenols and Alcohols. Linear regression parameters for the correlation between p_xp_y -type MO energies and pK_a values are shown in Table 8.⁸² The F value used for the Fisher Test was 7.88 for 23 degrees of freedom and a 99% confidence level.

The results with p_xp_y -type MO energies are much better than those obtained with HOMO energies (Table 6). In fact, HOMO energies are not adequate for describing the acid–base character of alcohols and phenols as a single family. Instead, we need to use the p_xp_y -type MO energies for this correlation, as it can be seen in Figure 7. Plots A and B show the correlations between pK_a and HOMO (A) or p_xp_y -type MO (B) energies at the HF level. Plot C shows the correlation between pK_a and HOMO energies, and plot D shows the correlation for pK_a values with p_xp_y -type MO energies. Both plots C and D are for calculations at the DFT level. It is clear from plots A and C that the alkoxide and phenoxide ions do not behave as a coherent group, they rather behave as two different groups. However, when the p_xp_y -type MO energies are used, their acid–base behavior is united. Moreover, the correlation results for the p_xp_y -type MOs confirms our hypothesis that the problem in using the HOMO to describe the acid–base behavior for phenol and alcohol anions is related to the influence of the aromatic π -electrons on the HOMO for phenoxide ions.

We have seen that solvent effects are extremely important in order to correctly describe the acid–base behavior of carbox-

TABLE 8: Linear Regression Parameters for pK_a Values vs p_xp_y -Type MO Energy^a Plots for Phenoxide and the Alkoxide Ions

| methodology | r^2 | a^b | b^c | pK_a error | SD ^d | F |
|-----------------------|-------|--------------|------------|--------------|-----------------|--------|
| HF/6-31G(d,p) | 0.953 | 65.1 (7.9) | 21.6 (1.3) | 1.80 | 0.676 | 464.7 |
| HF/COSMO/6-31G(d,p) | 0.981 | 138.8 (7.3) | 61.7 (2.7) | 0.81 | 0.431 | 1173.9 |
| HF/COSMO/6-31+G(d,p) | 0.971 | 154.7 (9.6) | 71.0 (3.7) | 0.95 | 0.532 | 762.5 |
| DFT/6-31G(d,p) | 0.918 | 75.1 (11.3) | 11.1 (0.4) | 2.20 | 0.893 | 256.3 |
| DFT/COSMO/6-31G(d,p) | 0.979 | 165.5 (8.4) | 43.7 (1.7) | 0.79 | 0.456 | 1049.2 |
| DFT/COSMO/6-31+G(d,p) | 0.959 | 222.8 (13.6) | 62.9 (3.2) | 0.95 | 0.631 | 537.0 |

^a Values for orbitals energies in Hartrees. ^b Angular coefficient. The number in parentheses is the standard error. ^c Linear coefficient. The number in parentheses is the standard error. ^d SD = standard deviation or root-mean-square deviation. $F_{1,23} = 7.88$, 99% confidence level.

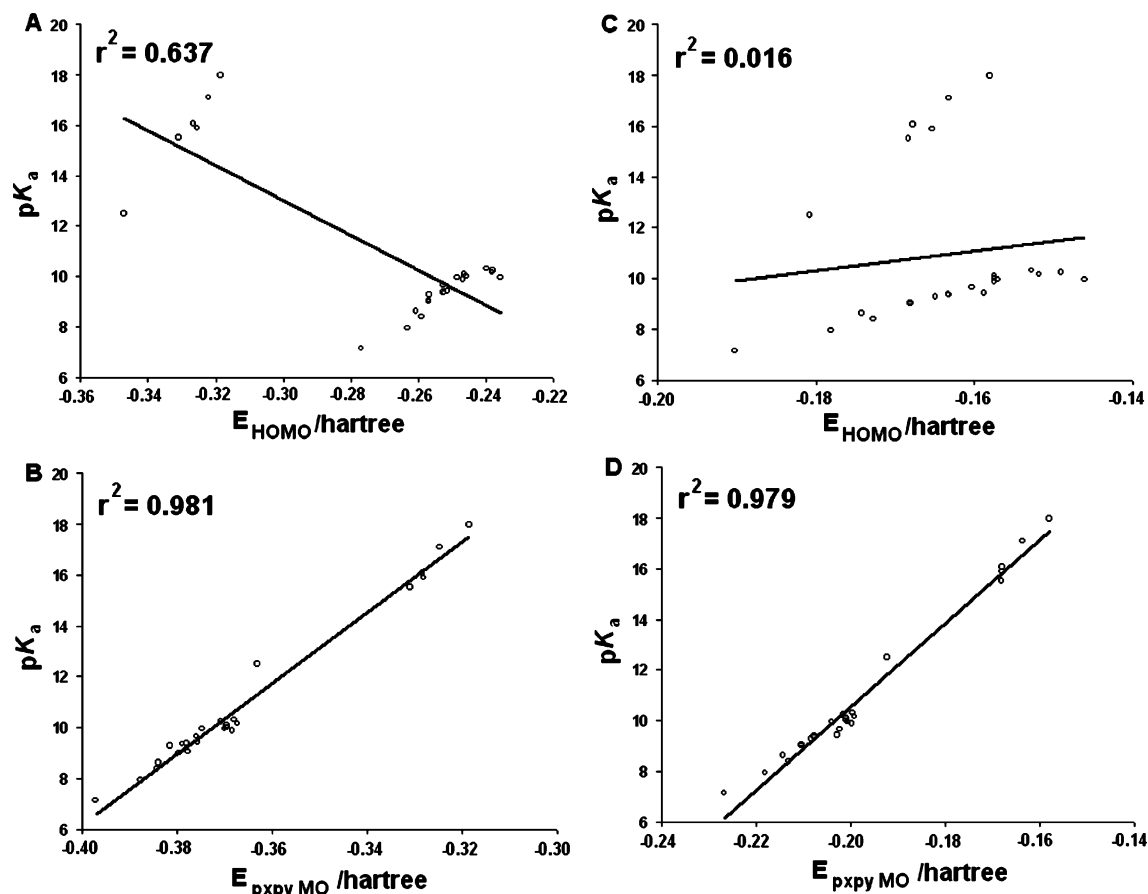


Figure 7. Plots for the correlation between phenols and alcohols pK_a values and their anions MO energies (in hartree). (A) HF HOMO; (B) HF p_xp_y -type MO; (C) DFT HOMO; (D) DFT p_xp_y -type MO. MO energies for plots A and B were calculated at the HF/COSMO/6-31G(d,p) level and for plots C and D were calculated at the DFT/COSMO/6-31G(d,p) level.

ylate ions. For phenoxide and alkoxide ions, the solvent effects have a smaller, but still important role. By analysis of the data, we can observe that the methodologies that do not include solvent effects, HF/6-31G(d,p) and DFT/6-31G(d,p), provided good r^2 values but poor standard deviations and pK_a errors. As we have noticed for phenoxide ions, solvent effects could be neglected (see Table 7), and since they form the majority of the compounds of this class, the lack of solvent effects on phenoxide ions is observed for the whole collection of compounds. On the other hand, all of the alkoxide ions studied showed a strong dependence on solvent effects, and an improvement in their correlation parameters leads to an improvement for the collection. This amelioration of the correlation parameters is relatively small only because the number of alkoxide ions in the whole collection is small.

4.3. MO Composition. As previously stated, the frontier MO that drives the acid–base reaction must be mainly located at the atom or group of atoms where the reaction takes place. In other words, the main contribution to this frontier MO must come from the reactive atom or group of atoms. Therefore, for carboxylate ions, the MO whose acid–base behavior we are trying to describe is mainly formed by orbitals from the carboxylate group (COO^-). Similarly, for phenoxide and alkoxide ions, the MO must be mainly composed of orbitals originated from the oxygen atom of the OH group. We have calculated, using the procedure described by Solomon and co-workers,⁶³ the MO composition for the methodologies that gave the best correlation parameters. For carboxylate ions, the MO composition was calculated by the DFT/COSMO/6-31+G(d,p) methodology and for phenoxide and alkoxide ions by the HF/COSMO/6-31G(d,p) methodology.

For carboxylate ions, the frontier MO with the largest COO^- contribution are always p_z - or p_xp_y -type ones. Moreover, if one of them has the largest COO^- contribution, the other has the second largest COO^- contribution, and only some exceptions to this rule were observed (**5**, **6**, **8**, **13**, **17**, **21**, and **24**). We already know that p_xp_y -type MOs are the best frontier MO to describe the acid–base behavior of carboxylic acids and its conjugated bases. One could also expect that these orbitals should have the largest COO^- contribution. Although p_xp_y -type MOs were not always the frontier MO with largest COO^- composition, we have seen that their spatial position, at the same plane of the COO^- , is decisive in this case.

Compared to carboxylic acids, phenols and alcohols are simpler systems. Consequently, the MO composition works well for them. In this case, the p_xp_y -type MO has the largest oxygen contribution for all phenoxide ions. For alkoxide ions, the HOMO (p_z -type) and p_xp_y -type MOs are very close to the percentage of oxygen orbital contribution, the largest difference being 5.90%.⁸² The energy difference between them is also small. Hence, for the studied alkoxide ions, the HOMO and p_xp_y -type MOs have extremely little differences for all purposes, meaning that any of these two MOs can be the one used to describe their acid–base behavior.

The MO composition itself cannot predict the correct reactive MO, as it is the case for carboxylic acids, but this is a practical tool that helps one to find the probable reactive MO. We can conclude that the MO composition in combination with the MO shape is the criterion to determine the MO that drives a reaction.

In his Nobel lecture, Fukui stated that the HOMO–LUMO approach could, sometimes, fail.⁹⁰ For those cases, he suggested that “any occupied orbitals which are very close to HOMO

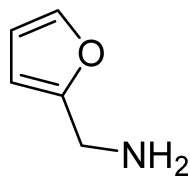


Figure 8. Furfurylamine molecule.

should properly be taken in account". Thus, when the HOMO fails, another frontier MO would be responsible for the phenomenon. Therefore, an important point here is to define what a frontier MO is. We carried out the calculation of the MO composition for the five last HOMOs. However, it does not imply that these five MOs are frontier MO ones. For example, the methoxide ion has only nine occupied MOs. Therefore, five occupied MOs are more than 50% of all occupied MOs. On the other hand, *p*-bromobenzoate ion has 49 occupied MOs, where five occupied MOs are only 10.2% of all occupied MOs. Clearly, there are no rules to establish the number of frontier MOs of a molecule. However, anyone shall agree that five frontier MOs for a small molecule as the methoxide ion seems an exaggerated number. On the other hand, larger molecules, with larger number of electrons, could have more than five frontier MOs. Thus, it is difficult to build a rule to identify how many frontier MOs a molecule has.

How can we find the orbital that is "very close to the HOMO"? This information is crucial to better understand the role of MOs in chemistry. Reactions involving donation and acceptance of electrons are related to MO energies, since electrons are occupying and will occupy a MO and a frontier one, as stated by Fukui. What we have done in this study was to build a criterion to determine the frontier effective-for-reaction molecular orbital, which we will abbreviate as FERMO.

The FERMO concept is a simple but also a necessary tool. With the FERMO concept, reactions that were not driven by HOMO–LUMO properties are no longer exceptions. We have seen, for two groups of compounds, the conjugated bases of carboxylic acids and phenols/alcohols, that HOMO energies cannot describe their acid–base behavior. However, those compounds are not exceptions: their HOMOs simply do not have the adequate shape and composition to correlate with their pK_a , as the p_xp_y -type MOs have. Therefore, the p_xp_y -type MOs are the FERMOs for the acid–base reaction. Without our criterion, it would be very difficult to find those FERMO because their relative energy varies with the calculation method used.

We can imagine some molecules with two different reaction sites, for example, a Lewis base bonded to a chain with an unsaturated bond. Some reactions can take place with participation of the electron pair from the Lewis base (a nucleophilic attack for example), while different reactions can occur with participation of the unsaturated bond (a Diels–Alder reaction for example). Could the same MO drive reactions that are so different? Probably two different MOs will drive those different reactions.⁹¹ The reactions involving the Lewis base will have a FERMO and the reactions with the unsaturated bond will have another FERMO. An example is the reaction between furfuryl-amines and citraconic anhydride.⁹² In this reaction, the furan moiety act as a diene in a Diels–Alder reaction and the amine moiety attacks the carbonyl groups of the citraconic anhydride. The furfurylamine (Figure 8) MO composition shows clearly the FERMO for each reaction. The diene moiety of the furan ring has the largest contribution for the HOMO (91.2% for HF method and 77% for DFT). On the other hand, the nitrogen contribution from the amine moiety is larger in the second

HOMO for DFT calculations (66.1%) and in the third HOMO for HF calculations (74.2%). Thus, the FERMO for the Diels–Alder reaction is the HOMO and the FERMO for the reaction between the amine and the carbonyl groups is another frontier molecular orbital.

Therefore, there are clear limitations on the HOMO–LUMO approach, and other concepts are needed to complement HOMO–LUMO arguments. The RHO procedure, developed by Hirao, Owhada, and co-workers,^{32–35,93} and the FERMO concept, developed in this work, can be used to solve these limitations and better explain the chemical behavior of molecules.

5. Conclusion

We stated a criterion to identify if the HOMO, or another frontier MO, is the effective MO for a given reaction, introducing the FERMO concept. In this work we used the FERMO in order to obtain a good correlation between the acidity and molecular orbital energies for a collection of carboxylic acids, phenols, and alcohols conjugated bases. The use of the FERMO concept made the unification of the acid character of phenols and alcohols possible, thus showing that this is a general concept. In principle, the FERMO can be used to understand reactions that the HOMO–LUMO approach did and did not explain, thus making stronger the role of MO theory in chemistry. Moreover, the HF and DFT results point toward the same MO as being the FERMO. This result, along with other studies,^{59,60,71} have shown that KS orbitals are more than a simple mathematical tool since they often display the same behavior from that observed for HF orbitals. It is also important to stress that, independent of their relative energies, we were able to identify the FERMO using our criterion, which is based on the MO shape, location, and composition.

Although calculation of the pK_a was not an objective of this work, the best linear models obtained here can be used for this purpose. It is interesting to notice that MO energies are sensitive to solvent effects and these effects play an important role in acid–base chemistry. We also found that the COSMO model gave better results than the PCM model and that there is a clear dependence between the basis set and the calculation method. In our calculations, we used the approximation that the vacuum and the solvated geometries are the same, thus making possible the improvement of the correlations if solvent effects are considered during the geometry optimization. Those effects are now under investigation.

Acknowledgment. We gratefully acknowledge the financial support given by CNPq, CAPES, and FAPERJ. We also acknowledge professor Peter Politzer from University of New Orleans who kindly sent us copies of his papers.^{59,61}

Supporting Information Available: Cartesian coordinates, MO energies, and MO energy orders for all of the compounds used in this work at all calculations levels used are available. The results for linear correlations using other methodologies (PCM results) and the MO composition for carboxylate ions (DFT/COSMO/6-31+G(d,p)) and for phenoxide and alkoxide ions (HF/COSMO/6-31G(d,p)) are provided. This material is available free of charge via the Internet at <http://pubs.acs.org>.

References and Notes

- (1) Hehre, W. J.; Random, L.; Schleyer, P. v. R.; Pople, J. A. *Ab Initio Molecular Orbital Theory*; John Wiley & Sons: New York, 1986.
- (2) Jorgensen, W. L.; Briggs, J. M. *J. Am. Chem. Soc.* **1989**, *111*, 4190–4197.

- (3) Lim, C.; Bashford, D.; Karplus, M. *J. Phys. Chem.* **1991**, *95*, 5610–5620.
- (4) Chen, J. L.; Noodleman, L.; Case, D. A.; Bashford, D. *J. Phys. Chem.* **1994**, *98*, 11059–11068.
- (5) Li, G. S.; Ruiz-López, M. F.; Maigret, B. *J. Phys. Chem. A* **1997**, *101*, 7885–7892.
- (6) Schüürmann, G.; Cossi, M.; Barone, V.; Tomasi, J. *J. Phys. Chem. A* **1998**, *102*, 6706–6712.
- (7) Silva, C. O.; Silva, E. C.; Nascimento, M. A. C. *J. Phys. Chem. A* **1999**, *103*, 11194–11199.
- (8) Silva, C. O.; Silva, E. C.; Nascimento, M. A. C. *J. Phys. Chem. A* **2000**, *104*, 2404–2409.
- (9) Liptak, M. D.; Shields, G. C. *J. Am. Chem. Soc.* **2001**, *123*, 7314–7319.
- (10) Toth, A. M.; Liptak, M. D.; Phillips, D. L.; Shields, G. C. *J. Chem. Phys.* **2001**, *114*, 4595–4606.
- (11) Liptak, M. D.; Gross, K. C.; Seybold, P. G.; Feldgus, S.; Shields, G. C. *J. Am. Chem. Soc.* **2002**, *124*, 6421–6427.
- (12) Chipman, D. M. *J. Phys. Chem. A* **2002**, *106*, 7413–7422.
- (13) Adam, K. R. *J. Phys. Chem. A* **2002**, *106*, 11963–11972.
- (14) Klamt, A.; Eckert, F.; Diedenhofen, M.; Beck, M. E. *J. Phys. Chem. A* **2003**, *107*, 9380–9386.
- (15) Pytela, O.; Otyepka, M.; Kulhánek, J.; Otyepková, E.; Nevěčná, T. *J. Phys. Chem. A* **2003**, *107*, 11489–11496.
- (16) Namazian, M.; Heidary, H. *THEOCHEM* **2003**, *620*, 257–263.
- (17) Chaudry, U. A.; Popelier, P. L. A. *J. Org. Chem.* **2004**, *69*, 233–241.
- (18) Fu, Y.; Liu, L.; Li, R.; Liu, R.; Guo, Q. *J. Am. Chem. Soc.* **2004**, *126*, 814–822.
- (19) Brinck, T.; Murray, J. S.; Politzer, P. *J. Org. Chem.* **1991**, *56*, 5012–5015.
- (20) Gross, K. C.; Seybold, P. G.; Peralta-Inga, Z.; Murray, J. S.; Politzer, P. *J. Org. Chem.* **2001**, *66*, 6919–6925.
- (21) Ma, Y.; Gross, K. C.; Hollingsworth, C. A.; Seybold, P. G.; Murray, J. S. *J. Mol. Model.* **2004**, *10*, 235–239.
- (22) Gross, K. C.; Seybold, P. G. *Int. J. Quantum Chem.* **2000**, *80*, 1107–1115.
- (23) Gross, K. C.; Seybold, P. G. *Int. J. Quantum Chem.* **2001**, *85*, 569–579.
- (24) Hollingsworth, C. A.; Seybold, P. G.; Hadad, C. M. *Int. J. Quantum Chem.* **2002**, *90*, 1396–1403.
- (25) Gruber, C.; Buss, V. *Chemosphere* **1989**, *19*, 15–95.
- (26) Machado, H. J. S.; Hinchliffe, A. *THEOCHEM* **1995**, *339*, 255–258.
- (27) Citra, M. J. *Chemosphere* **1999**, *38*, 191–206.
- (28) Soriano, E.; Cerdán, S.; Ballesteros, P. *THEOCHEM* **2004**, *684*, 121–128.
- (29) Fujimoto, H.; Mizutani, Y.; Iwaze, K. *J. Phys. Chem.* **1986**, *90*, 2768–2772.
- (30) Fujimoto, H. *Acc. Chem. Res.* **1987**, *20*, 448–453.
- (31) Omoto, K.; Fujimoto, H. *J. Am. Chem. Soc.* **1997**, *119*, 5366–5372.
- (32) Hirao, H.; Ohwada, T. *J. Phys. Chem. A* **2003**, *107*, 2875–2881.
- (33) Nakamura, S.; Hirao, H.; Ohwada, T. *J. Org. Chem.* **2004**, *69*, 4309–4316.
- (34) Ohwada, T.; Hirao, H.; Ogawa, A. *J. Org. Chem.* **2004**, *69*, 7486–7494.
- (35) Hirao, H.; Ohwada, T. *J. Phys. Chem. A* **2005**, *109*, 816–824.
- (36) Szabo, A.; Ostlund, N. S. *Modern Quantum Chemistry. Introduction to Advanced Electronic Structure Theory*; McGraw-Hill Publishing Company: New York, 1989.
- (37) Itatani, J.; Levesque, J.; Zeidler, D.; Niikura, H.; Pépin, H.; Kieffer, J. C.; Corkum, P. B.; Villeneuve, D. M. *Nature* **2004**, *432*, 867–871.
- (38) Koopmans, T. A. *Physica* **1933**, *1*, 104–113.
- (39) Fukui, K.; Yonezawa, T.; Shingu, H. *J. Chem. Phys.* **1952**, *20*, 722–725.
- (40) Fukui, K.; Yonezawa, T.; Nagata, C.; Shingu, H. *J. Chem. Phys.* **1954**, *22*, 1433–1442.
- (41) Woodward, R. B.; Hoffmann, R. *J. Am. Chem. Soc.* **1965**, *87*, 395–397.
- (42) Hoffmann, R.; Woodward, R. B. *J. Am. Chem. Soc.* **1965**, *87*, 2046–2048.
- (43) Woodward, R. B.; Hoffmann, R. *J. Am. Chem. Soc.* **1965**, *87*, 2511–2513.
- (44) Hoffmann, R.; Woodward, R. B. *J. Am. Chem. Soc.* **1965**, *87*, 4388–4389.
- (45) Hoffmann, R.; Woodward, R. B. *J. Am. Chem. Soc.* **1965**, *87*, 4389–4390.
- (46) Hoffmann, R.; Woodward, R. B. *Acc. Chem. Res.* **1968**, *1*, 17–22.
- (47) Woodward, R. B.; Hoffmann, R. *Angew. Chem.* **1969**, *81*, 797–870.
- (48) Salem, L. *J. Am. Chem. Soc.* **1968**, *90*, 543–552.
- (49) Salem, L. *J. Am. Chem. Soc.* **1968**, *90*, 553–566.
- (50) Houk, K. N. *Acc. Chem. Res.* **1975**, *8*, 361–369.
- (51) Fujimoto, H.; Sugiyama, T. *J. Am. Chem. Soc.* **1977**, *99*, 15–22.
- (52) Fujimoto, H.; Inagaki, S.; *J. Am. Chem. Soc.* **1977**, *99*, 7424–7432.
- (53) Pearson, R. G. *J. Am. Chem. Soc.* **1963**, *85*, 3533–3539.
- (54) Klopman, G. *J. Am. Chem. Soc.* **1968**, *90*, 223–234.
- (55) Pearson, R. G. *J. Am. Chem. Soc.* **1986**, *108*, 6109–6114.
- (56) Hohenberg, P.; Kohn, W. *Phys. Rev.* **1964**, *136*, B864–B871.
- (57) Kohn, W.; Sham, L. J. *Phys. Rev.* **1965**, *140*, A1133–A1138.
- (58) Kohn, W.; Becke, A. D.; Parr, R. G.; *J. Phys. Chem.* **1996**, *100*, 12974–12980.
- (59) Politzer, P.; Abu-Awwad, F. *Theor. Chem. Acc.* **1998**, *99*, 83–87.
- (60) Baerends, E. J.; Gritsenko, O. V. *J. Phys. Chem.* **1997**, *101*, 5383–5403.
- (61) Politzer, P.; Abu-Awwad, F.; Murray, J. S.; *Int. J. Quantum Chem.* **1998**, *69*, 607–613.
- (62) Brunold, T. C.; Gamelin, D. R.; Solomon, E. I. *J. Am. Chem. Soc.* **2000**, *122*, 8511–8523.
- (63) Chen, P.; Fujisawa, K.; Solomon, E. I. *J. Am. Chem. Soc.* **2000**, *122*, 10177–10193.
- (64) Randall, D. W.; George, S. D.; Hedman, B.; Hodgson, K. O.; Fujisawa, K.; Solomon, E. I. *J. Am. Chem. Soc.* **2000**, *122*, 11620–11631.
- (65) Randall, D. W.; George, S. D.; Holland, P. L.; Hedman, B.; Hodgson, K. O.; Tolman, W. B.; Solomon, E. I. *J. Am. Chem. Soc.* **2000**, *122*, 11632–11648.
- (66) Cheng, P.; Solomon, E. I. *Inorg. Biochem.* **2002**, *88*, 368–374.
- (67) Skulan, A. J.; Hanson, M. A.; Hsu, H.; Dong, Y.; Que, L., Jr.; Solomon, E. I. *Inorg. Chem.* **2003**, *42*, 6489–6496.
- (68) Schenk, G.; Pau, M. Y. M.; Solomon, E. I. *J. Am. Chem. Soc.* **2004**, *126*, 505–515.
- (69) Basumallick, L.; Sarangi, R.; George, S. D.; Elmore, B.; Hooper, A. B.; Hedman, B.; Hodgson, K. O.; Solomon, E. I. *J. Am. Chem. Soc.* **2005**, *127*, 3531–3544.
- (70) Savin, A.; Umrigar, C. J.; Gonze, X. *Chem. Phys. Lett.* **1998**, *288*, 391–395.
- (71) Stowasser, R.; Hoffmann, R. *J. Am. Chem. Soc.* **1999**, *121*, 3414–3420.
- (72) Frisch, M. J., et al. *Gaussian 98*, revision A.11; Gaussian, Inc.: Pittsburgh, PA, 2001.
- (73) Becke, A. D. *J. Chem. Phys.* **1993**, *98*, 5648–5652.
- (74) Lee, C.; Yang, W.; Parr, R. G. *Phys. Rev. B* **1988**, *37*, 785–789.
- (75) Miertuš, S.; Scrocco, E.; Tomasi, J. *Chem. Phys.* **1981**, *55*, 117–129.
- (76) Miertuš, S.; Tomasi, J. *Chem. Phys.* **1982**, *65*, 239–245.
- (77) Cossi, M.; Barone, V.; Cammi, R.; Tomasi, J. *Chem. Phys. Lett.* **1996**, *255*, 327–335.
- (78) Klamt, A.; Schüürmann, G. *J. Chem. Soc., Perkins Trans.* **1993**, *2*, 799–805.
- (79) Barone, V.; Cossi, M. *J. Phys. Chem. A* **1998**, *102*, 1995–2001.
- (80) We are using the orbital shapes instead of orbital symmetries for two main reasons. First, since we did not constrain the symmetry in the calculations, all but few molecules belong to C1 group and the orbital symmetries are *n_a*, where *n* is the orbital number. Second, the orbital symmetry group does not help us find the orbital location in a molecule (although in other cases the symmetry does). Thus, we must check their shapes to have this information. In this particular case, the orbital shape gives more useful information than symmetry does.
- (81) Skoog, D. A.; West, D. M.; Holler, F. J. *Analytical Chemistry. An Introduction*; Saunders College Publishing: 1994.
- (82) See Supporting Information for complete results.
- (83) Box, G. E. P.; Hunter, W. G.; Hunter, J. S. *Statistics for Experiments. An Introduction to Design, Data Analysis, and Model Building*; John Wiley & Sons: 1978.
- (84) We are using the *p_z*- and *p_xp_y*-type MO notation just for convenience. The real meaning here is that *p_xp_y*-type MO is mainly formed by any two *p* atomic orbitals (not necessarily the *p_x* and *p_y*) and the *p_z* ones by the remaining *p* atomic orbital.
- (85) We thank the reviewers for this discussion.
- (86) Edward, J. T. *J. Chem. Educ.* **1982**, *59*, 354–356.
- (87) Compound **35** has a difference between the regression and calculated MO energy higher than four times the standard deviation.
- (88) Exner, O.; Böhm, S. *J. Org. Chem.* **2002**, *67*, 6320–6327.
- (89) Exner, O.; _ársky, P. *J. Am. Chem. Soc.* **2001**, *123*, 9564–9570.
- (90) Fukui, K. *Angew. Chem., Int. Ed. Engl.* **1982**, *21*, 801–809.
- (91) If the molecule is too small, it is possible that only one MO could drive different reactions.
- (92) Murali, R.; Scheeren, H. W. *Tetrahedron Lett.* **1999**, *40*, 3029–3032.
- (93) Hirao, H.; Ohwada, T. *J. Phys. Chem. A* **2005**, *109*, 7642–7647.